

This article was downloaded by: [National Chiao Tung University 國立交通大學]
On: 28 April 2014, At: 04:19
Publisher: Taylor & Francis
Informa Ltd Registered in England and Wales Registered Number: 1072954
Registered office: Mortimer House, 37-41 Mortimer Street, London W1T 3JH,
UK



Aerosol Science and Technology

Publication details, including instructions for authors and subscription information:

<http://www.tandfonline.com/loi/uast20>

Factors Influencing Pressure Drop through a Dust Cake during Filtration

Yu-Hsiang Cheng^a & Chuen-Jinn Tsai^a

^a Institute of Environmental Engineering, National Chiao Tung University, No. 75, Poai St., Hsin Chu, Taiwan, Republic of China

Published online: 13 Jun 2007.

To cite this article: Yu-Hsiang Cheng & Chuen-Jinn Tsai (1998) Factors Influencing Pressure Drop through a Dust Cake during Filtration, *Aerosol Science and Technology*, 29:4, 315-328, DOI: [10.1080/02786829808965572](https://doi.org/10.1080/02786829808965572)

To link to this article: <http://dx.doi.org/10.1080/02786829808965572>

PLEASE SCROLL DOWN FOR ARTICLE

Taylor & Francis makes every effort to ensure the accuracy of all the information (the "Content") contained in the publications on our platform. However, Taylor & Francis, our agents, and our licensors make no representations or warranties whatsoever as to the accuracy, completeness, or suitability for any purpose of the Content. Any opinions and views expressed in this publication are the opinions and views of the authors, and are not the views of or endorsed by Taylor & Francis. The accuracy of the Content should not be relied upon and should be independently verified with primary sources of information. Taylor and Francis shall not be liable for any losses, actions, claims, proceedings, demands, costs, expenses, damages, and other liabilities whatsoever or howsoever caused arising directly or indirectly in connection with, in relation to or arising out of the use of the Content.

This article may be used for research, teaching, and private study purposes. Any substantial or systematic reproduction, redistribution, reselling, loan, sub-licensing, systematic supply, or distribution in any form to anyone is expressly forbidden. Terms & Conditions of access and use can be found at <http://www.tandfonline.com/page/terms-and-conditions>



Factors Influencing Pressure Drop through a Dust Cake during Filtration

Yu-Hsiang Cheng and Chuen-Jinn Tsai*

INSTITUTE OF ENVIRONMENTAL ENGINEERING, NATIONAL CHIAO TUNG UNIVERSITY, No. 75,
POAI ST., HSIN CHU, TAIWAN, REPUBLIC OF CHINA

ABSTRACT. Three kinds of dust materials, fly ash (MMAD : 6.28 μm), limestone (MMAD : 2.53 μm) and SAE fine dust (MMAD : 3.88 μm), have been used to test the dust cake compaction and its influence on the specific dust cake resistance coefficient at filtration velocity ranging from 1 to 9 cm/sec. An accurate laser displacement system was used to determine dust cake thickness and the amount of dust cake compaction during filtration. In the range of filtration velocity tested, dust cake compaction has been found to occur. Higher filtration velocity results in larger amount of irreversible dust cake compaction and lesser amount of elastic dust cake compaction. The experimental specific dust cake resistance coefficient, K_2 , has also been found to increase with an increasing filtration velocity. For the three dusts tested, K_2 relates to filtration velocity V_f as $K_2 \propto V_f^n$, where n is 0.52, 0.38 and 0.43, for fly ash, limestone and SAE fine dust respectively. The theoretical K_2 values predicted by the Rudnick-Happel equation has been shown to agree better with the experimental K_2 values than those by the Kozeny-Carman equation. The maximum difference between the K_2 values predicted by the Rudnick-Happel equation and the experimental values is less than about 16%. AEROSOL SCIENCE AND TECHNOLOGY 29:315-328 (1998) © 1998 American Association for Aerosol Research

INTRODUCTION

Filtration velocity, V_f , has been found to affect the magnitude of specific dust cake resistance coefficient, K_2 (Spaite and Walsh, 1963; Borgwardt and Durham, 1967; Dennis and Durham, 1979; Dennis and Dirgo, 1981). Most previous researchers have reported that the relationship between K_2 and V_f is $K_2 = fV_f^n$, where f and n are constants. The constant n is always positive, indicating that higher filtration velocity always results in greater K_2 . A wide range of n exists in the literature. Experimental data of Spaite and Walsh (1963) show that n is about 0.5 for

both mica and fly ash, despite that particle shape between mica (roughly plate-like) and fly ash (roughly spherical) is quite different. Other experimental data have shown that n is 0.75 for fly ash (Borgwardt and Durham, 1967); 0.19 for submicron Arizona road dust (Rudnick and First, 1978a and 1978b); 0.5 for coal fly ash (Dennis et al., 1979; Dennis and Dirgo, 1981). These results show that dust cake will be compacted to a greater extent when subjected to a higher fluid drag force leading to smaller dust cake porosity and greater K_2 at higher filtration velocity, (VanOsdell et al., 1984; Klemm et al., 1980).

Rudnick and First (1978a, 1978b) also indicated that dust cake compaction was due

*Corresponding author.

mainly to increasing pressure drop as dust cake thickened. But, the amount of compaction of the dust cake with respect to filtration velocity and its influence on the K_2 value remained to be determined. In particular, an accurate system to measure the amount of compaction of the dust cake has yet to be developed.

The theoretical method to estimate the K_2 value is based upon filtration theory. The Kozeny-Carman equation has been used widely to calculate the pressure drop across dust cake deposited on a filtration medium. This semiempirical equation also may be used to predict K_2 value based on dust cake porosity and an empirical constant. Rudnick and First (1978a, 1978b) provided an equation that derived from the Happel's cell model (1958) to predict K_2 without an empirical constant. K_2 values predicted by the classical Kozeny-Carman equation and by the Rudnick-Happel equation agree to within $\pm 20\%$ over the dust cake porosity ranging from 0.3 to 0.7. When the dust cake porosity is greater than 0.7, the Rudnick-Happel equation always predicts higher K_2 values than those computed by the Kozeny-Carman equation. Dennis and Dirgo (1981) measured K_2 values of several fly ashes at the laboratory and compared them with the predicted values by the Rudnick-Happel equation. The predicted values were found to be three times greater than the measured values.

Most previous theories are unable to predict K_2 values accurately, because errors may occur when measuring parameters such as dust cake porosity or particle size distribution (Dennis et al., 1979; Dennis and Dirgo, 1981). To account for the polydispersity of the particulate material, volume-surface mean diameter (also called Sauter diameter) was usually used to represent the particle size of the lognormally distributed dust for calculating specific dust cake resistance coefficient. Gupta et al. (1993) used the Rudnick-Happel equation to predicted K_2 values. The results were shown to be in good agreement with the experimental data for nonhygroscopic aluminum oxide for the dust cake porosity ranging from 0.84 to 0.95.

However, for the hygroscopic sodium chloride, the agreement was shown to be poor due to large variation in the dust cake porosity measurement.

The previous review points out there are substantial differences between experimental data as well as theoretical predictions in the property and specific resistance coefficient of the dust cake. The incapability of measuring porosity and compressibility of the dust cake accurately under different filtration conditions seems to be one of the major factors that leads to these discrepancies. There is a critical need to measure the porosity and compressibility of the dust cake accurately using different dust materials at different filtration velocities. Current theoretical models for K_2 should be reexamined using reliable experimental data under well-controlled conditions.

In this study, laboratory measurement was conducted to obtain K_2 values for three kinds of dust cakes: fly ash, limestone, and SAE fine dust, at different filtration velocities. After the dust cake was formed, an accurate laser displacement system was used to measure the thickness of dust cake and to obtain its porosity. Then the experimental K_2 values were compared with theoretical predictions at filtration velocity ranging from 1 to 9 cm/sec.

FUNDAMENTAL THEORY OF K_2

When there is a significant particle mass loaded on a filter, total pressure drop across the filter can be expressed as the sum of the pressure drop across the clean filter medium, ΔP_f , and that across the dust cake, Δp_c , as follows

$$\Delta P = \Delta P_f + \Delta P_c \quad (1)$$

From Darcy's law, ΔP_f can be written as the filtration velocity times the filter resistance constant K_1 as

$$\Delta P_f = K_1 V_f \quad (2)$$

where K_1 depends upon the physical characteristics of the filter medium such as the

filter pore size, filter material and filter thickness.

The pressure drop across the dust cake can be derived from the drag force across all individual particles. It also can be described by Darcy's law as a function of the specific dust cake resistance coefficient, K_2 , the dust mass deposited, M , the filtration velocity, V_f , and the filtration area, A , as

$$\Delta P_c = \frac{\Sigma F_D}{A} = K_2 \frac{V_f M}{A} = K_2 V_f W \quad (3a)$$

or

$$S = \frac{\Delta P_c}{V_f} = K_2 W \quad (3b)$$

where W is the mass areal density of the dust cake and S is the filter drag. If the drag force F_D exerted on each particle by the airflow is governed by the Stokes law, the above equation can be expressed as

$$\Delta P_c = \frac{\Sigma F_D}{A} = \frac{3\pi\mu V_f}{A} \Sigma \frac{N_i D_{pi}}{C_i} \quad (4)$$

where N is the total particle number in the dust cake, μ is the gas viscosity, D_p is the particle size, and C is the Cunningham slip correction factor.

If particles are monodisperse and isolated, then Eq. (4) can be written as

$$\Delta P_c = \frac{18\mu}{\rho_p D_p^2 C} \frac{V_f M}{A} = K_{2st} \frac{V_f M}{A} \quad (5)$$

where K_{2st} is the theoretical specific dust cake resistance coefficient for separate, isolated and monodisperse spherical particles.

To account for the fact that particles are in contact with each other, and are polydis-

perse, different researchers have developed methods to calculate the specific dust cake resistance coefficient such as the Kozeny-Carman equation or the Rudnick-Happel equation (Happel, 1958; Rudnick and First, 1978a, 1978b; Gupta et al., 1993).

Kozeny and Carman derived a semiempirical equation that represents the dust cake as a series of parallel capillaries or channels whose total volume equals the void volume of the cake and whose surface area equals the surface area of the particles constituting the cake. The specific dust cake resistance coefficient is defined as a function of the dust cake porosity ϵ as

$$K_{2k-c} = \frac{18\mu}{\rho_p D_{VS}^2 C} \frac{2k(1-\epsilon)}{\epsilon^3} \quad (6)$$

where the empirical constant k is equal to 4.8 for spherical particles and 5.0 for irregular particles, the D_{VS} is the volume-surface mean diameter (or Sauter diameter).

Rudnick and First (1978a, 1978b) described an equation for specific dust cake resistance coefficient that derived from the Happel's cell model (1958) to predict pressure drop across a dust cake without an empirical constant. The Happel's cell model treats the dust cake as an assemblage of individual particles, each cell containing a particle surrounded by an imaginary concentric spherical shell. The porosity of the dust cake is equal to the ratio of the volume between the spherical shell and the particle to that of the spherical shell. The specific dust cake resistance coefficient based on the Happel's cell model and reformulated by Gupta et al. (1993) can be expressed as

$$K_{2R-H} = \frac{18\mu}{\rho_p D_{pg}^2 C} \exp(-4.0 \ln^2 \sigma_g) \frac{3 + 2(1-\epsilon)^{5/3}}{3 - 4.5(1-\epsilon)^{1/3} + 4.5(1-\epsilon)^{5/3} - 3(1-\epsilon)^2} \quad (7)$$

In this model, D_{pg} is the geometric mean diameter for polydisperse dusts, and slip correction factor, C , is calculated based on D_{pg} (Gupta et al., 1993).

However, these equations require a knowledge of the dust cake porosity and

particle size distribution. The dust cake porosity is often difficult to estimate theoretically or experimentally due to the complexity of cake structure. This study improves the experimental method to measure the dust cake porosity, the particle size distribution

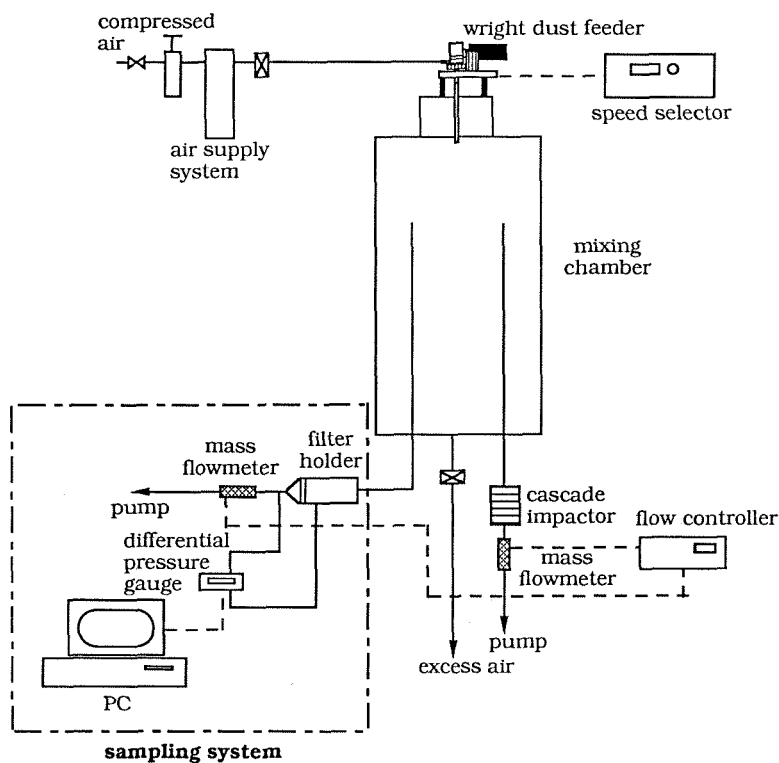


FIGURE 1. Schematic diagram of the experimental setup for dust filtration.

and the specific dust cake resistance coefficient under well-controlled conditions. The experimental K_2 values then will be compared with theoretical predictions by different models, Eqs. (6) and (7).

EXPERIMENTAL METHOD

An experimental system shown in Fig. 1 was designed to measure the pressure drop as a function of sampling time or mass areal loading (mass per unit area of filter, M/A). Three test dusts, fly ash (obtained from the Hsin-Da coal-fired power plant, Taiwan), limestone (Lih Hsiang Industrial Co., Japan), and SAE fine dust (Power Technology Inc., Burnsville, MN, USA) were used in this study. A Wright dust feeder (WDF-II, BGI Inc., Waltham, MA, USA) was used to generate the test dust, which was introduced into a dust chamber. The dust chamber is 35

cm in diameter and 50 cm in height. The dust chamber has two sampling tubes which are 45 cm long. The inner diameter of the sampling tube is 1.05 cm. One sampling tube was connected to a Marple personal cascade impactor (Model 225-50-001, SKC Inc., Eighty Four, PA, USA) to measure the particle size distribution of the test dust, while another one was connected to the filtration system using a 90° elbow. The cutoff aerodynamic diameters of the Marple cascade impactor are 21.3, 14.8, 9.8, 6.0, 3.5, 1.55, 0.93, and 0.52 μm respectively for each stage at the sampling flow rate of 2.0 L/min. In this study, particles were found to deposit on the filter uniformly which allowed the thickness of the dust cake to be measured accurately.

The filtration system includes a filter holder, a digital manometer, a mass flowmeter, and an IBM PC. The diameter of the filter collection area was designed to be 3.5

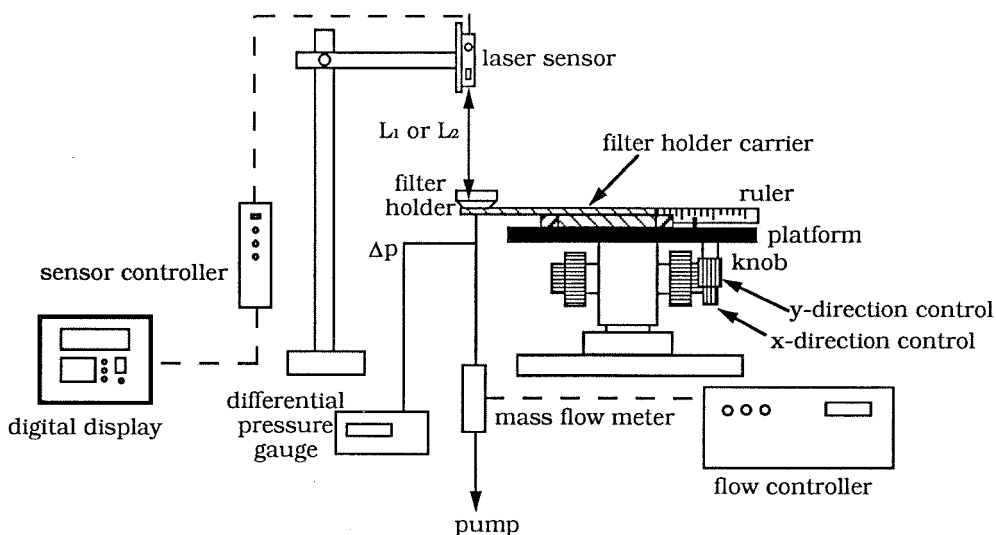


FIGURE 2. Schematic diagram of the laser displacement sensor system.

cm. A straight tube that is 8 cm long and 3.5 cm in diameter was connected carefully before the filter holder to keep the air velocity and deposited particles uniform on the filter surface. The pressure drop across the filter holder was measured using a digital differential pressure gauge, and the signal of the pressure drop was recorded with an IBM PC continuously. The constant filtration velocity through the filter was controlled by a mass flowmeter. Filtration velocities used in this study were 1.0, 3.0, 6.0, and 9.0 cm/sec, which corresponded to sampling flow rates of 0.58, 1.73, 3.46, and 5.20 L/min.

The dust concentration in the chamber was controlled by the rotational speed of the dust feeder and the flow rate of the compressed air. In this study, the revolution speed of the Wright dust feeder was kept at 0.8 RPM, and the inlet pressure of compressed air was controlled at 6 psig. At these operating conditions, the mass concentration was about 1.36 ~ 1.96 g/m³ for fly ash, 2.83 ~ 3.40 g/m³ for limestone, and 2.78 ~ 3.72 g/m³ for SAE fine dust respectively. Test particles generated by the dust feeder might carry electrostatic charge. However, the effect of electrostatic charge on dust cake properties was not studied.

The particle size distribution of the dust was measured twice with the cascade impactor at each run. The impactor sampling time took about 15 to 20 sec to avoid overloading of the cascade impactor stages. The particle loss in the sampling tube and the filtration system was taken into account by considering diffusion, impaction, sedimentation and turbulent deposition mechanisms (Liu et al., 1985).

To investigate dust cake porosity, a measurement system shown in Fig. 2 was designed. A laser displacement sensor (Model LB-72/LB-12, Keyence Corp., Takatsuki, Osaka, Japan) was used to measure the distance between the laser sensor and the filter surface or dust cake surface. The sensor was mounted on a support that was fixed on a laboratory desk. The resolution of this laser displacement sensor is 2 mm. Before dust sampling, the blank filter was weighted for its blank weight M_1 . Then, this filter was installed into the filter holder, supported by a stainless screen, and mounted on a removable platform. The distance between the sensor and the clean filter surface was determined while clean air was flowing through the filter at a designated filtration velocity to minimize measurement errors. The baseline

TABLE 1. Measured Particle Size, Geometric Standard Deviation, Porosity of Dust Cake, and Specific Dust Cake Resistance Coefficient for Test Dusts

Material	V_f (cm/sec)	MMAD (μm)	σ_g	$\epsilon \pm \text{SD}$	$K_2 \pm \text{SD}$ (S^{-1})
Fly Ash	1	5.72	2.11	0.82 ± 0.01	87500 ± 5300
	3	6.01	1.91	0.70 ± 0.01	169000 ± 15000
	6	6.67	2.05	0.61 ± 0.02	24000 ± 7900
	9	6.71	2.07	0.52 ± 0.02	263000 ± 7400
Limestone	1	2.37	1.93	0.86 ± 0.01	380000 ± 42000
	3	2.53	2.06	0.77 ± 0.03	506000 ± 23000
	6	2.60	2.12	0.74 ± 0.01	736000 ± 22000
	9	2.60	2.11	0.68 ± 0.01	872000 ± 41000
SAE	1	3.34	2.03	0.84 ± 0.01	227000 ± 12000
	3	3.78	2.16	0.79 ± 0.01	306000 ± 20000
	6	4.18	2.33	0.73 ± 0.01	479000 ± 49000
	9	4.20	2.35	0.66 ± 0.01	570000 ± 67000

distance, L_1 , was calculated as the average of measurements at 18 points evenly distributed on the filter. It was noted that the filter support must be firm enough to avoid deformation when the air was drawn through the filter. After measuring the baseline distance, the filter holder was removed from the platform and was assembled in the filtration system. It was found that the coefficient of variation of thickness measurement was about 3%, indicating the reliability of current experimental method.

The ΔP -t curve then was obtained by sampling test dust through the filter at a constant filtration velocity. Total filtration time was recorded after an uniformed dust cake was formed. Typically, a uniform dust layer was formed on the filter when the mass areal density was greater than 0.02 g/cm^2 for limestone and SAE fine dust, and 0.04 g/cm^2 for fly ash. After sampling, the filter holder was disassembled from the filtration system without turning off the sampling pump. The dust cake otherwise would fracture when the pump was turned off. The filter holder with dust loaded filter was reinstalled on the platform to measure the distance, L_2 , between the sensor and the dust cake surface. Again, L_2 was the average of 18 measurements on the dust cake surface. To study dust cake compaction by filtering air, changes of the pressure drop and the cake thickness were recorded while the cake was subjected to dust-free air at a certain face velocity, which

was lower or higher than the filtration velocity used to form the dust cake.

After measuring the thickness of the dust cake L , which was calculated as $L = L_1 - L_2$, the dust loaded filter was disassembled from the filter holder and weighted again to obtain the weight of dust loaded filter, M_2 . The total mass areal density on the filter, W_T , was calculated as $W = (M_2 - M_1)/A$. The dust cake porosity was then determined as

$$\epsilon = 1 - \frac{W}{\rho_p L} \quad (8)$$

The particle densities of fly ash, limestone, and SAE fine dust are 2.06 g/cm^3 , 2.70 g/cm^3 , and 2.65 g/cm^3 respectively, as obtained from the manufacturers or suppliers.

After the experiment, the ΔP -t data was transformed into the S-W data. The experimental K_2 value was determined as the slope of the linear portion of the S-W curve by linear regression. The linear portion of the S-W curve corresponds to the condition when an uniform dust cake is formed.

RESULTS AND DISCUSSION

Measured data of particle mass median aerodynamic diameter (MMAD), geometric standard deviation (σ_g), dust cake porosity (ϵ), and specific dust cake resistance coefficient (K_2), for fly ash, limestone, and SAE fine dust at different filtration velocities are

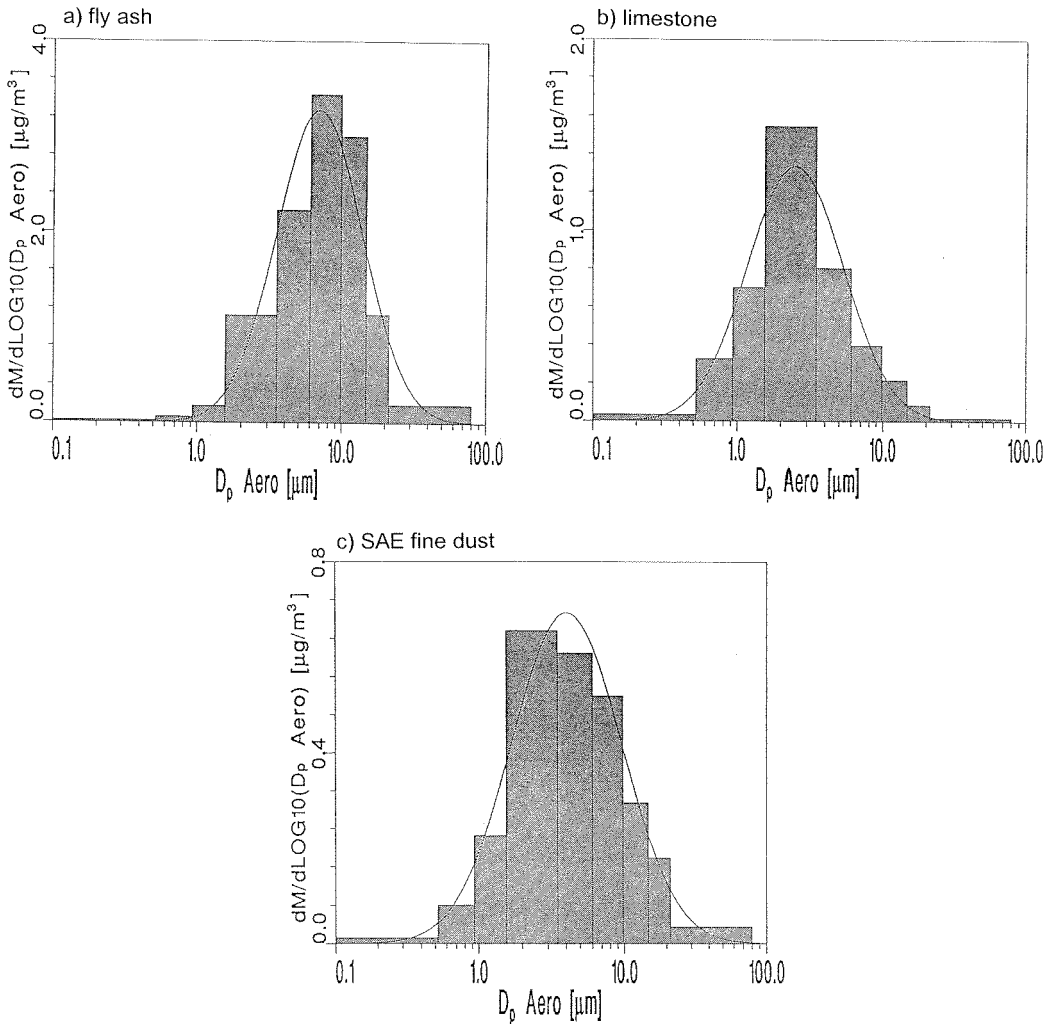


FIGURE 3. Typical measured particle size distributions at the filtration velocity of 9 cm/sec. (a) fly ash, MMAD = 6.71 μm , $\sigma_g = 2.07$ (b) limestone, MMAD = 2.60 μm , $\sigma_g = 2.11$ (c) SAE fine dust, MMAD = 4.20 μm , $\sigma_g = 2.35$. The solid curves and fitting parameters, MMAD and σ_g , were obtained using DISFIT program.

shown in Table 1. Each data is the average of four to five test runs. In the dust chamber, the temperature was kept at $26 \pm 1^\circ\text{C}$, and the relative humidity was below 10%. The MMAD and σ_g for the test dusts loaded on the filter were measured and corrected for particle loss in the transport tubes of the cascade impactor and filtration system. Figs. 3a–3c show the typical particle size distribution for fly ash, limestone and SAE fine dust,

respectively, at the filtration velocity of 9 cm/sec. Solid curves in the figures were obtained by fitting the data using DISFIT program distributed by TSI Inc. (St. Paul, MN, USA). The MMAD of the loaded dusts on the filter was found to be smaller than that in the test chamber mainly due to particle loss in the transport tube of the filtration line. It was found that loss due to large particle sedimentation in the horizontal tube of the

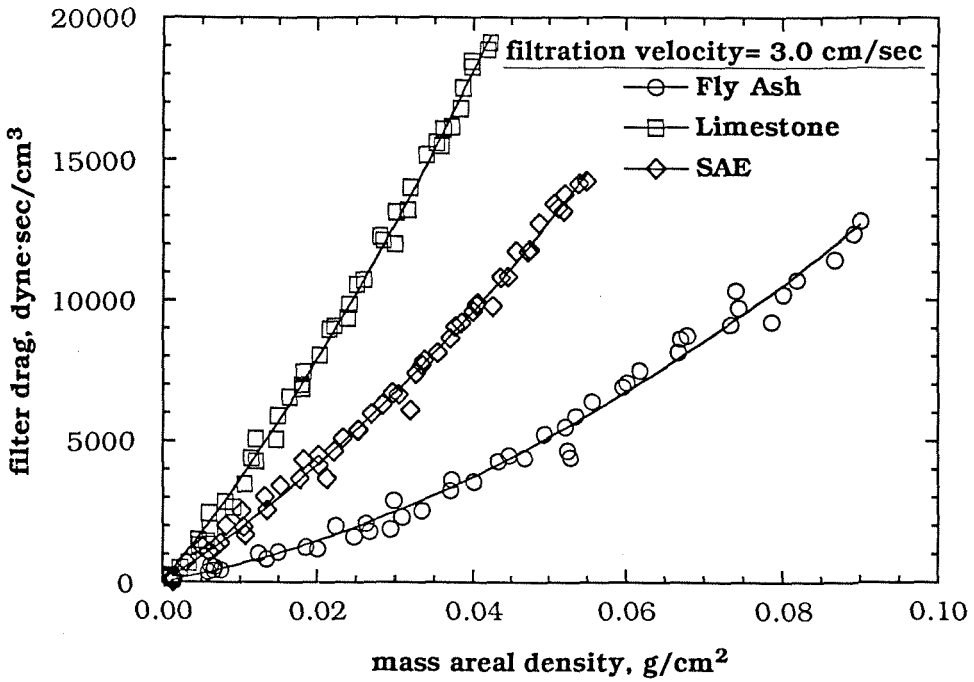


FIGURE 4. Filter drag versus mass areal density for fly ash, limestone and SAE fine dust at the filtration velocity of 3.0 cm/sec.

filtration system was severe when the filtration velocity was low. This led to a smaller MMAD for smaller filtration velocity as shown in Table 1. Average MMAD for different filtration velocities for fly ash, limestone, and SAE fine dust is 6.28, 2.53, and 3.88 mm respectively.

The S-W curve can be divided into two regions: initial cake developing region and uniform cake region. In the initial region, the filter drag increases as particles are captured on the filter. The increase of filter drag is dependent on the initial filtration mechanisms, filter material, and particle characteristics. When a uniform dust cake forms on the filter, the filter drag increases linearly with mass areal density.

An example of the S-W curve is shown in Fig. 4 for fly ash, limestone, and SAE fine dust when the filtration velocity equals to 3 cm/sec. It can be seen that the S-W curve for fly ash has a clear initial region, but the region is not very obvious for limestone and

SAE fine dust. This is because when the pore diameter of the filter is small relative to particles size, the pores can be filled up faster at a given mass areal density (Gupta et al., 1993; Novick et al., 1992; Japuntich et al., 1994). In Table 1, it can be seen that the K_2 increases as particle size decreases. At the same filtration velocity, limestone has the highest K_2 since it is the smallest in size among the three dust materials. Also Table 1 shows that for the three test dusts tested, higher filtration velocity results in a smaller porosity but higher K_2 value.

Figure 5 shows the relationship between the filtration velocity and the dust cake porosity of fly ash, limestone, and SAE fine dust. It is seen that the dust cake porosity decrease with an increasing filtration velocity for all three test dusts. At higher filtration velocity, larger fraction of particles will be compressed deeper into the cake when fluid drag force overcomes particle adhesion force. Despite their smaller sizes, irregular

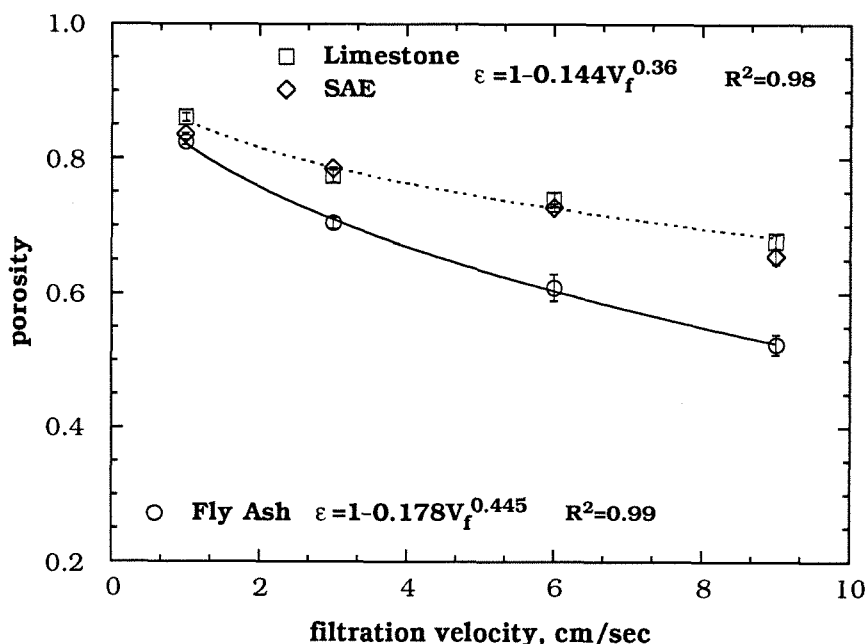


FIGURE 5. The relationship between filtration velocity and dust cake porosity for fly ash, limestone and SAE fine dust.

limestone, and SAE fine dust particle have larger dust cake porosity than spherical fly ash particles. The possible reason could be due to the more random arrangement of irregular particles in the dust cake than the spherical particles. This confirms that the dust cake porosity also depends on the shape of the particle. Two empirical equations to express the relationship between the filtration velocity and the dust cake porosity are developed as

$$\epsilon = 1 - 0.178 V_f^{0.445}, R^2 = 0.99, \text{ for fly Ash} \quad (9a)$$

$$\epsilon = 1 - 0.144 V_f^{0.36}, R^2 = 0.98, \text{ for Limestone and SAE} \quad (9b)$$

where the unit of V_f is cm/sec. These two empirical equations are suitable for filtration velocity ranging from 1 to 9 cm/sec. When determining the theoretical K_2 values, knowledge of the dust cake porosity and its dependence on filtration velocity, such as Eqs. (9a) and (9b), is very important.

The compaction characteristics of the dust cake was examined further by measuring the pressure drop across an uniform dust cake when it is subject to clean air at face velocities different from the filtration velocity used to form the dust cake. The results are shown in Figs. 6a – 6c for fly ash, limestone, and SAE fine dust respectively. In Fig. 6a, the dust cake was formed at filtration velocity of 3 cm/sec, where the pressure drop shown at point A in the figure is 2.6×10^4 dyne/cm². As the clean air is drawn through the cake at a face velocity smaller than 3 cm/sec, it is seen that the pressure drop decreases linearly with decreasing face velocity as shown by the dashed line AA'. This indicates the dust cake may expand elastically from that formed at higher filtration velocity. By increasing the face velocity from 1 cm/sec at point A' to 3 cm/sec at point A does not change the characteristic of the dust cake so that the pressure drop increases along the same dashed line A'A. This further confirms that the dust cake compaction is

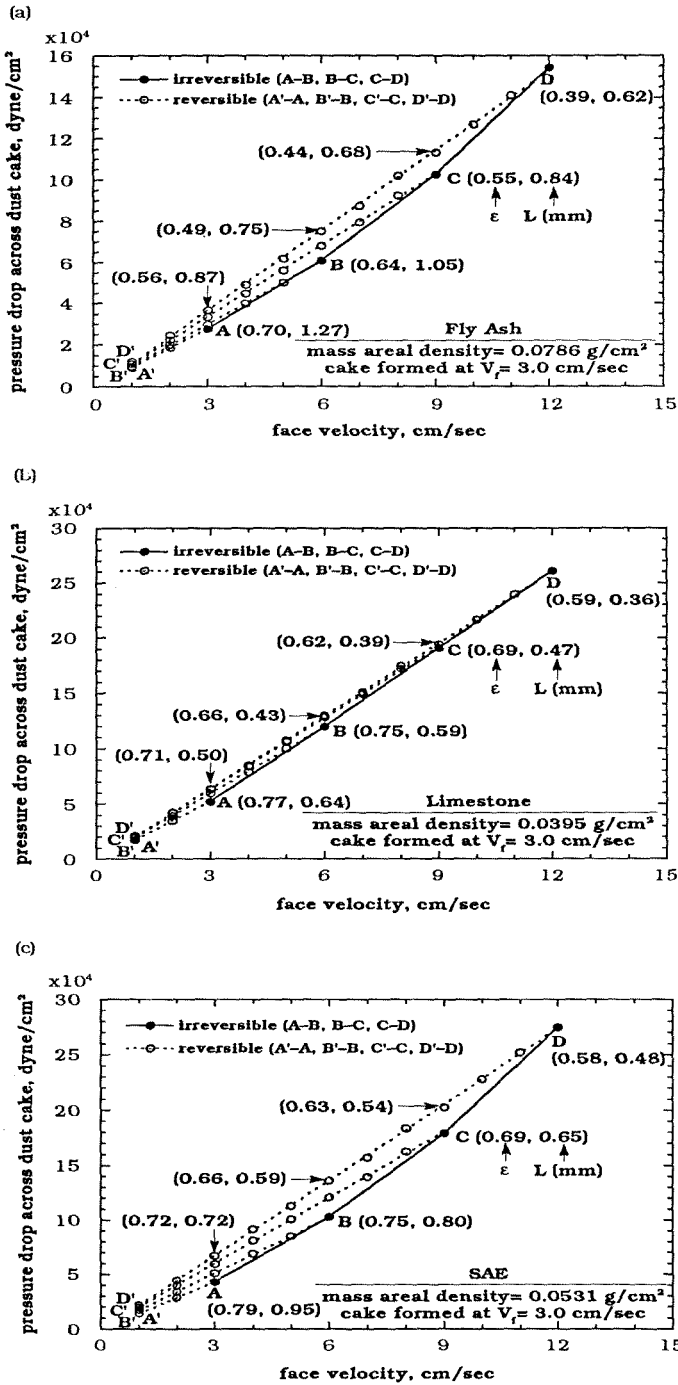


FIGURE 6. The compressibility characteristic of dust cake at different clean air face velocities. (a) fly ash, (b) limestone, (c) SAE fine dust. First and second number in the parenthesis is the porosity and thickness respectively.

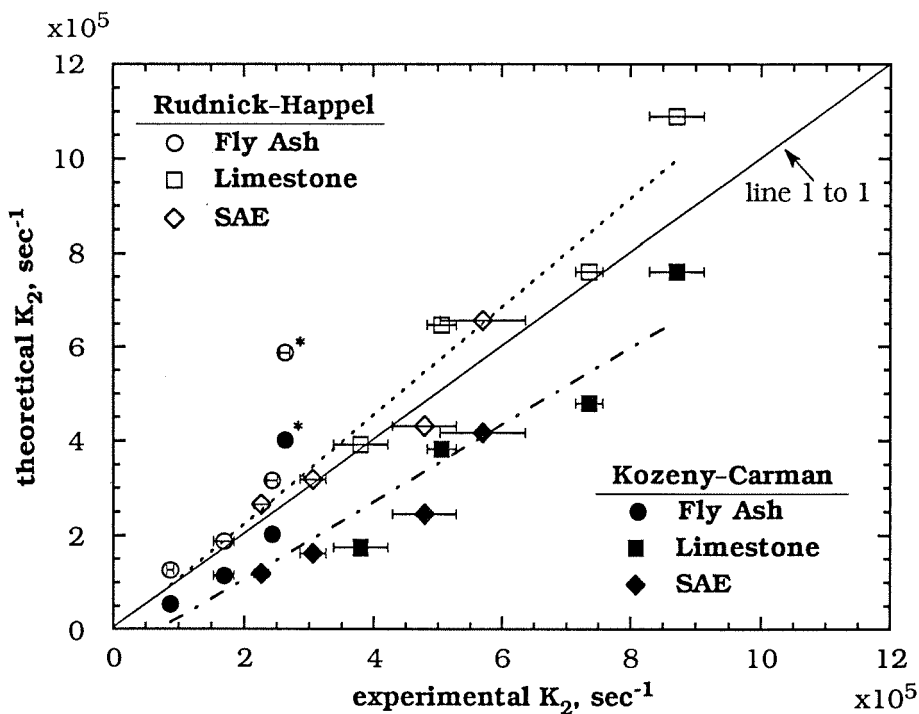


FIGURE 7. Comparison of the experimental K_2 values with theoretical predictions using Rudnick-Happel (open symbols) and Kozeny-Carman (filled symbols) equations. (*:exceptional data point for fly ash particles at the filtration velocity of 9 cm/sec)

elastic as long as the clean air face velocity is below the cake-forming filtration velocity.

However, if the clean air face velocity increases from 3 cm/sec (point A) to 6 cm/sec (point B), then the porosity of the dust cake becomes smaller as witnessed by a greater slope of line AB compared to that of line A'A. This observation is consistent with Fig. 5 that shows a similar trend that higher filtration velocity yields a less porous dust cake. Continuing the experiment by decreasing the clean air face velocity from 6 cm/sec (point B) to 1 cm/sec (point B') along BB', it is seen that the pressure drop decreases linearly with decreasing velocity. However, the slope of line BB' is greater than that of line AA', indicating that a portion of the dust cake may have been compacted irreversibly as face velocity increases from point A to B. Again, increasing the face velocity from B' to B does not change the slope of the pressure

drop line. This also indicates the recovery of the portion of the dust cake that is under elastic compaction. At even high face velocity, 12 cm/sec, similar compressibility characteristics can be observed in Fig. 6a. For limestone and SAE fine dust, similar behavior of dust cake compaction also appears as in Fig. 6b and 6c respectively.

It is important to have a proper K_2 model that predicts pressure drop accurately to facilitate the design of a baghouse. The porosity of the dust cake shown in Fig. 5 taking into account of the effect of filtration velocity was used to calculate the theoretical K_2 values by Rudnick-Happel equation, Eq. (7), and Kozeny-Carman equation, Eq. (6). In Eq. (6), the Sauter diameter D_{vs} was calculated as (Hinds, 1982)

$$D_{VS} = D_{MMD} \exp(-0.5 \ln^2 \sigma_g) \quad (10)$$

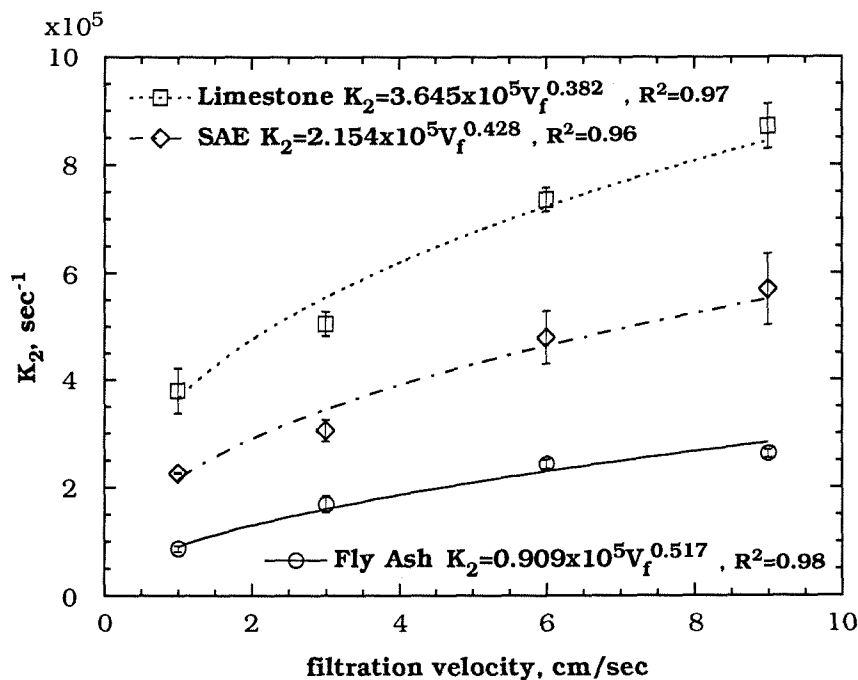


FIGURE 8. The relationship between filtration velocity and K_2 for fly ash, limestone and SAE fine dust.

Figure 7 compares the experimental K_2 values with theoretical predictions using Rudnick-Happel equation (open symbols) and Kozeny-Carman equation (filled symbols). Herein, it can be seen that the prediction of K_2 values by Rudnick-Happel equation is more accurate than the Kozeny-Carman equation. Excluding the data points for fly ash at the filtration velocity of 9 cm/sec, the Rudnick-Happel equation overestimates the experimental K_2 values by no more than 16% for the three tested dusts, which is much better than the Kozeny-Carman equation that underestimates the experimental K_2 by as much as 35%. Much greater overestimation of about 120% occurs for the Rudnick-Happel equation when the dust cake porosity is smaller than 0.6 for fly ash at the filtration velocity of 9 cm/sec. The exact reason why the Rudnick-Happel equation is unable to predict K_2 values at this high filtration velocity accurately is unknown. It is speculated that nonuniform po-

rosity distribution across the thickness of the cake may have occurred for the cake that is formed at high filtration velocity.

The relationship between the filtration velocity and the specific dust cake resistance coefficient, K_2 , for fly ash, limestone, and SAE fine dust are shown in Fig. 8. According to the experimental data, the relationship between the filtration velocity and the specific dust cake resistance coefficient, K_2 , for fly ash, limestone, and SAE fine dust can be expressed as

$$K_2 = 0.909 \times 10^5 V_f^{0.517}, R^2 = 0.98 \text{ for Fly Ash} \quad (11a)$$

$$K_2 = 3.645 \times 10^5 V_f^{0.382}, R^2 = 0.97 \text{ for Limestone} \quad (11b)$$

$$K_2 = 2.154 \times 10^5 V_f^{0.428}, R^2 = 0.96 \text{ for SAE} \quad (11c)$$

where the unit of V_f is cm/sec and that of K_2 is sec^{-1} . In this study, n for fly ash is found to 0.52, which is close to the values of Spaite and Walsh (1963) and Dennis and Dirgo (1981).

These three empirical equations are suitable for the filtration velocity ranging from 1 to 9 cm/sec and MMAD from 5 μm to 7 μm for fly ash, 2 μm to 3 μm for limestone, and 3 μm to 5 μm for SAE fine dust. From these equations, it can be seen that for fly ash, an increasing filtration velocity leads to more increase in K_2 than both limestone and SAE fine dust as is evident from the values of the exponent n . This is maybe due to the fact that spherical fly ash particles are more amenable to compaction than irregular limestone and SAE fine dust particles at a given filtration velocity. Such speculation can also be seen from Fig. 5 where it shows the change of the porosity with increasing filtration velocity for fly ash is more drastic than that of limestone and SAE fine dust.

CONCLUSIONS

This study has investigated the dust cake porosity, specific dust cake resistance coefficient, and compressibility of dust cake for fly ash, limestone, and SAE fine dust. Laboratory experimental system has been set up to facilitate accurate measurement of the dust cake porosity. It has been found that K_2 increases as particle size decreases, or when the filtration velocity increases. At the same filtration velocity, limestone has the highest K_2 since it is the smallest in size among the three dust materials.

From the experimental results, the dust cake is seen to be irreversibly compressed during filtration. The fraction of the dust cake undergoes irreversible compaction is seen to increase with increasing filtration velocity. At higher filtration velocity, the dust cake is compacted more resulting in a smaller dust cake porosity and a larger K_2 value.

Despite their smaller sizes, irregular limestone and SAE fine dust particles have larger dust cake porosity than spherical fly ash particles. The possible reason could be due to

the more random arrangement of irregular particles in the dust cake than the spherical particles.

In this study, the prediction of K_2 values by Rudnick-Happel equation is more accurate than the Kozeny-Carman equation. The Rudnick-Happel equation overestimates the experimental K_2 by no more than 16% for the three dusts tested.

The authors would like to thank the Taiwan National Science Council of the Republic of China for the financial support under Contract No. NSC 85-2211-E-009-012.

References

- Borgwardt, R. H., and Durham, J. F. (1967). Factors Affecting the Performance of Fabric Filters. Paper presented at the 60th Annual Meeting of the American Institute of Chemical Engineers, New York, Nov. 29.
- Dennis, R., and Dirgo, J. A. (1981). Comparison of Laboratory and Field Derived K_2 Values for Dust Collected on Fabric Filters, *Filtration and Separation* 18:394-417.
- Dennis, R., Klemm, H. A., and Battye, W. (1979). *Fabric Filter Model Sensitivity Analysis*. GCA/Technology Division, EPA-600/7-79-043c, pp. 40-51.
- Gupta, A., Novick, V. J., Biswas, P., and Monson, P. R. (1993). Effect of Humidity and Particle Hygroscopicity on the Mass Loading Capacity of High Efficiency Particulate Air Filters, *Aerosol Sci. and Technol.* 19:94-107.
- Happel, J. (1958). Viscous Flow in Multiparticle Systems: Slow Motion of Fluids Relative to Beds of Spherical Particles, *AIChE J.* 4:197-201.
- Hinds, W. C. (1982). *Aerosol Technology: Properties, Behavior, and Measurement of Airborne Particles*, Wiley, New York.
- Japuntich, D. A., Stenhouse, J. I. T., and Liu, B. Y. H. (1994). Experimental Results of Solid Monodisperse Particle Clogging of Fibrous Filters, *J. Aerosol Sci.* 25:385-393.
- Klemm, H. A., Dirgo, J. A., and Dennis, R. (1980). *Fabric Filtration Analyses for Three Utility Boiler Flyashes*. EPA-600/7-80-157.
- Liu, B. Y. H., Pui, D. Y. H., Rubow, K. L., and Szymanski, W. W. (1985). Electrostatic Effects

- in Aerosol Sampling and Filtration. *Ann. Occup. Hyg.* 29:251-269.
- McKenna, J. D., and Turner J. H. (1993). *Fabric Filter Baghouse I*, ETS, Inc., Roanoke, VA.
- Novick, V. J., Monson, P. R., and Ellison, P. E. (1992). The Effect of Solid Particle Mass Loading on the Pressure Drop of HEPA Filters, *J. Aerosol Sci.* 23:657-665.
- Rudnick, S. N., and First, M. W. (1978a). *Third Symposium on Fabric Filters for Particulate Collection*, EPA-600/7-78-007, pp. 251-288.
- Rudnick, S. N., and First, M. W. (1978b). *Proceedings of the 71st Annual Meeting of the Air Pollution Control Association*, Paper No. 78-62.7, June 25-30, Houston, Texas.
- Spaite, R. H., and Walsh, G. W. (1963). Effect of Fabric Structure on Filter Performance. *Amer. Ind. Hyg. Assoc. J.* 24: 357-365.
- VanOsdell, D. W., Donovan, R. P., Furlong, D. A., and Hovis, L. S. (1984). *Fourth Symposium on the Transfer and Utilization of Particulate Control Technology*, EPA-600/9-84-025a, pp.342-356.

Received July 18, 1997; accepted June 1, 1998.